

C. Gil, A. Barbuti, P. Spuig, A. Boboc, S. Dorling
and JET EFDA contributors

Analysis and Improvements of Fringe Jump Corrections by Electronics on the JET Tokamak FIR Interferometer

“This document is intended for publication in the open literature. It is made available on the understanding that it may not be further circulated and extracts or references may not be published prior to publication of the original when applicable, or without the consent of the Publications Officer, EFDA, Culham Science Centre, Abingdon, Oxon, OX14 3DB, UK.”

“Enquiries about Copyright and reproduction should be addressed to the Publications Officer, EFDA, Culham Science Centre, Abingdon, Oxon, OX14 3DB, UK.”

The contents of this preprint and all other JET EFDA Preprints and Conference Papers are available to view online free at www.iop.org/Jet. This site has full search facilities and e-mail alert options. The diagrams contained within the PDFs on this site are hyperlinked from the year 1996 onwards.

Analysis and Improvements of Fringe Jump Corrections by Electronics on the JET Tokamak FIR Interferometer

C. Gil¹, A. Barbuti¹, P. Spuig¹, A. Boboc², S. Dorling²
and JET EFDA contributors*

JET-EFDA, Culham Science Centre, OX14 3DB, Abingdon, UK

¹*Association EURATOM-CEA, 13108 St Paul-lez-Durance, France*

²*EURATOM-UKAEA Fusion Association, Culham Science Centre, OX14 3DB, Abingdon, OXON, UK*

** See annex of F. Romanelli et al, "Overview of JET Results",
(Proc. 22nd IAEA Fusion Energy Conference, Geneva, Switzerland (2008)).*

Preprint of Paper to be submitted for publication in Proceedings of the
18th High Temperature Plasma Diagnostics, Wildwood, New Jersey, USA.
(16th May 2010 - 20th May 2010)

ABSTRACT.

For the Tore Supra interferometer phase measurements, CEA developed electronics using FPGA processors. The embedded algorithm can correct the fringe jumps. For comparison, the electronics ran at JET during the 2009 campaign. A first analysis concluded that the electronics was not correcting all the fringe jumps. Analysis of the failures led to improvements in the algorithm, which was tested during the rest of the campaign. In this article, we evaluate the performance increases. From the analysis of the remaining faults, further improvements are discussed for designing future boards that are foreseen for JET, using the second wavelength and the Cotton Mouton effect information.

1. INTRODUCTION

To diagnose the line-electron density of magnetic fusion hot plasmas, FIR interferometers [1] have been developed by means of plasma traversing beams in the wavelength range of 100-200 microns for the CEA Tore Supra [2-4] and the JET tokamaks [5]. The diagnostics of the two machines are very similar. They both use the principle of recombination of a 100KHz frequency shifted beam with the probe beam that has traversed the plasma. The interference produces a 100KHz signal, of which one can measure the phase change that is proportional to the line density. A reference beam outside the plasma allows a differential phase measurement. As the expected line density can reach $5 \times 10^{22} \text{ m}^{-2}$ in the tokamaks, the corresponding FIR beam phase changes are several 2π radians, commonly named fringes.

Thus, one needs to build up a dedicated electronics that continuously measures the phase, not to be lost in the counting of the fringes. However, at these wavelengths, losses of signal may happen, due to changes of trajectories when the FIR beams are crossing too strong density gradient plasmas. This configuration can occur during ELMs, disruptions or when pellets are injected in the plasma. The loss of the phase information can mislead the phase measurement and generate the so called fringe jumps, each jump corresponding to an error of roughly 10^{19} m^{-2} .

JET and CEA developed different electronics that both enable to reach a very good precision of the order of $3 \times 10^{17} \text{ m}^{-2}$. The JET method is based on a 400KHz sampling of the 100KHz signal, which allows reconstruction of the sinusoid and the corresponding phase. When the signal amplitude is lower than 90 mV, the phase measurement is stopped [5]. On Tore Supra, the sinusoidal signal is first transformed into a square signal, the ascending fronts of it being generated at every zero crossing of the sinusoid. The electronics thereafter counts the time delay between each front. Recently, the initial analogue design has been replaced by a numerical one. The program of the delay counting is now embedded in a Field Programmable Gate Array (FPGA) processor. When the amplitude is below a threshold (0.2 volt), the fronts disappear while an algorithm maintains the phase at the most plausible value [6]. This set up has been successfully installed on Tore Supra since 2007 and correctly calculates the phase when the signal is lost as for instance during ICRH break downs, although the measurement is still disturbed by disruptions or sometimes pellet injections.

2. ANALYSIS OF THE MEASUREMENTS

In order to test the electronics on different plasmas scenarios and prepare future developments, a complete rack of the CEA electronics has been installed in parallel with the JET electronics and connected to the vertical channels 3 and 4 (195 micron beams) during the 2009 campaign from Pulse No s 76103 to 79853.

Figure 1 shows that during a pulse, the evolutions of the measured phases of the two electronics are similar. However both of them encounter fringe jumps that lead to a Non Zero Final Value (NZFV). A statistical analysis on the first part of the campaign [7] confirmed that the number of NZFV was practically the same with the two electronics (Figure 2). None of the pulses with disruption led to a NZFV. The percentage of NZFV on the others pulses is 21% (resp. 40%) for channels 3 (resp.4). The failures in correcting the fringe jumps principally occur on pulses with ELM s.

To analyse the causes of the failures, we used the available JET 1MHz data acquisition to characterize the 100 KHz signal and to calculate the phase with exactly the same algorithm as the FPGA embedded one.

Figure 3 shows the amplitude and the phase simulations during an ELM. As there is no gas injection here, the phase should be the same before and after the disturbance.

One can see that the initial algorithm stops the phase counting while the signal amplitude is below the 0.2V threshold. It misses the phase increase but not the decrease, leading to a fringe jump. In contrast, the algorithm with a blocking period avoids this effect to give the right phase value after the ELM.

3. IMPROVEMENTS OF THE ALGORITHM

This algorithm with a 1ms blocking period has been compared on 324 JET pulses with the initial one. Figure 4 shows a statistics FIG 4: Diminution of the final phase by the improved algorithm based on the number of fringes counted after a pulse, which is indicative of the fringe jump correction efficiency.

One can see that the new algorithm better corrects the fringe jumps but still the number of NZFV remains significant. An analysis of the causes of the remaining failures with ELMs shows that in some cases the counting is stopped too late when the phase has already varied and that it would be advantageous to store a phase reference 1ms before the disturbing event and impose it when the signal loss occurs (Figure 5). By this method, the phase counting should completely avoid the transient density effect that is due to ELMs.

4. DISCUSSION ON THE FUTURE ELECTRONICS

As many diagnostics under present shutdown, the JET interferometer is undergoing at present a major upgrade. On the data acquisition side, CEA is in charge of designing a new electronics to elaborate the detected signal of the superimposed 119mm beams to the 195mm channels on the vertical system. The global electronic scheme will remain similar to the initial CEA design[6],

consisting of a zero crossing determination with a threshold amplitude method to detect the loss of signal and a numerical phase counting embedded in a FPGA processor. The algorithm, with a phase reference 1ms before the signal loss and a blocking period of 1ms after, will be implemented. Nevertheless, it is inefficient if the signal loss happens during a strong phase change due for instance to pellet injections. Some further algorithm improvements can be considered:

4.1. SECOND WAVELENGTH CORRECTION

The superposed 119 mm beam, as its wavelength is smaller, will be less sensitive to refraction and its diameter will be reduced in the ratio of the wavelengths. Thus one can expect it to be less sensitive to ELMs or pellet injections.

As the phase of the two wavelength signals will be calculated on the same FPGA board, information exchange between the two results will allow the validation of the phase measurements when signal losses are detected (Figure 6)

The proposed algorithm is straightforward: if a loss is detected on the second beam but not on the first one, the phase variation from a reference time will be calculated by the first one and applied to correct the second one at the restart of the counting. This hypothesis is valid if the phase variations of the two signals are due only to density change and thus are in the ratio of the wavelengths.

4.2. CORRECTION WITH THE ORTHOGONAL POLARIZATION SIGNAL

On the JET diagnostic, a free standing wire grid, which acts as a polarizer/analyzer in the FIR domain, separates the two orthogonal polarisation components of the 195mm infrared beam toward two distinct detectors. On the future FPGA board, additional inputs will be available to take advantage of information given by the orthogonal polarization signal to correct the fringe jumps of the first interferometric signal.

Even though the two orthogonal polarization signals could be lost simultaneously for a period, and thus have a wrong absolute phase at the restart of the counting after a signal loss, the correction could be done by evaluating the relative phase change between the two components, due to the Cotton Mouton effect [8]. As it is a small effect, the expected variation range is well below 2π radians, avoiding the fringe jump issue.

It is interesting to superpose the ellipticity and the phase, which are calculated by polarimetry, on the phase that is calculated by interferometry. On figure 7, one can see that the ellipticity roughly follows interferometric phase, except during the plasma ramp up and ramp down. During these phases, the ratio, in arbitrary units, between the two signals is not constant. On figure 8, the polarimetric phase shows strong discrepancy from the interferometric one, particularly during the transient plasma phases where the ratio dramatically decreases.

Nevertheless, as in principle the signals are proportional to density at least during short -typically less than 10 ms- periods, the following algorithm is proposed: the ratio between interferometric phase and polarimetric phase or ellipticity is continuously calculated while the amplitudes are

above the threshold. When a signal loss is detected, the phase variation is calculated using the last validated coefficient and then helps the correction of the interferometric phase at the restart of the counting. This algorithm has been partially validated in adding artificial fringe jumps and simultaneous density variations in the data (figures 7 and 8). By calculating the normalized relative variation between the interferometric phase and the polarimetric phase or ellipticity, one can see that the right coefficient is found for the event at 60s (bottom figures 7 and 8). Unfortunately this parameter is sometimes above one fringe even without any fringe jump. An analysis should be performed to understand the causes of this discrepancy and reduce it in order to be able to reliably correct the fringe jumps.

CONCLUSIONS

Thanks to the tests of the CEA electronics at JET, the algorithm to correct the fringe jumps has been improved and validated during the 2009 campaigns. The future electronics for JET will take into account the results of the tests. New correction algorithms are proposed for implementation in the future boards. Correction with the second wavelength phase will be possible. Correction by calculating the Cotton Mouton effect seems more difficult to achieve and further studies will analyse the causes of the discrepancies and reduce them.

ACKNOWLEDGMENTS

The authors want to thank D. Mazon and A. Murari for the Task Force D help to organize this task. This work, supported by the European communities under the contract of association between EURATOM and CEA, was carried out within the framework of the European Fusion Development Agreement. The views and opinions expressed herein do not necessarily reflect those of the European Commission.

REFERENCES

- [1]. D. Veron 1979 Infrared and millimeter waves (Button ed), **2**, chapter 2
- [2]. J.L. Bruneau and C.Gil,1989 Proceed.14th Conf. IRMMW in Wuzburg
- [3]. C. Gil, D. Elbeze, C. Portafaix, 2001 Fusion Engineering Design, **56-57** 969
- [4]. C. Gil, D. Elbeze, A. Beraud, B. Echard, J.C. Patterlini, J. Philip, L. Toulouse, M. Lipa, A. Litnovsky. 2007, Fusion Engineering Design, **82** 1238
- [5]. P. Innocente, D. Mazon, E. Joffrin, M. Riva 2003 Review of Scientific Instruments **74** 3645
- [6]. C. Gil, A. Barbuti, D. Elbeze, P. Pastor, J. Philip, L. Toulouse 2008 Review of Scientific Instruments **79** 10E710
- [7]. C. Gil, A. Boboc, A. Barbuti, P. Pastor 2009 LAPD conference, to be published in Journal of Physics: Conference Series
- [8]. M. Brombin, A. Boboc, A. Murari, E. Zilli, L. Giudicotti 2009 Review of Scientific Instruments **80** 063506

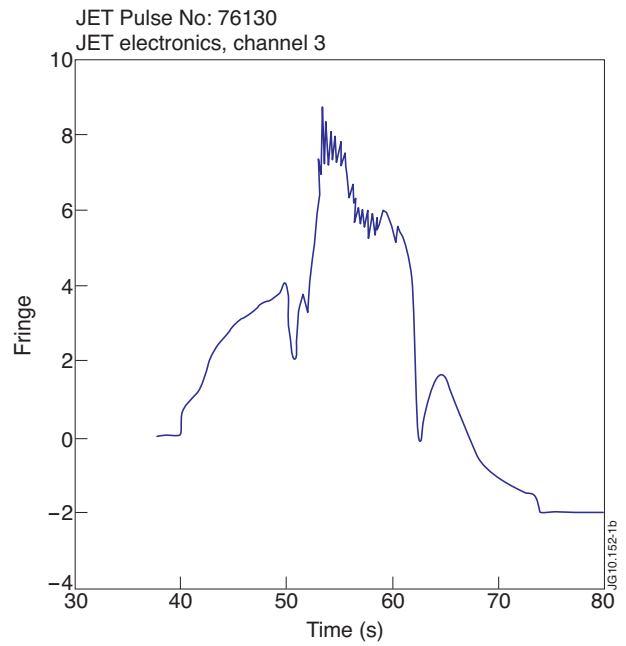
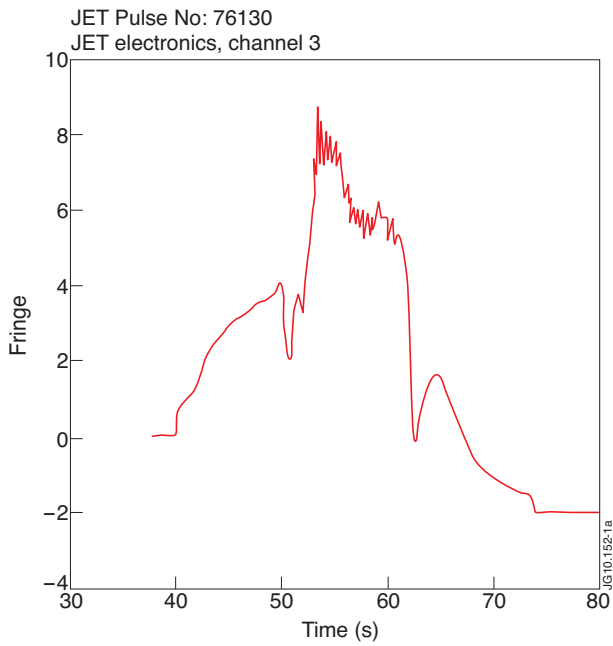


Figure 1: CEA and JET time evolution of the measured phases.

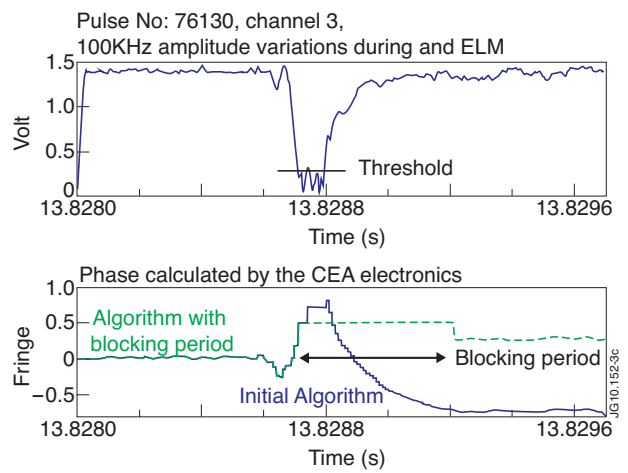
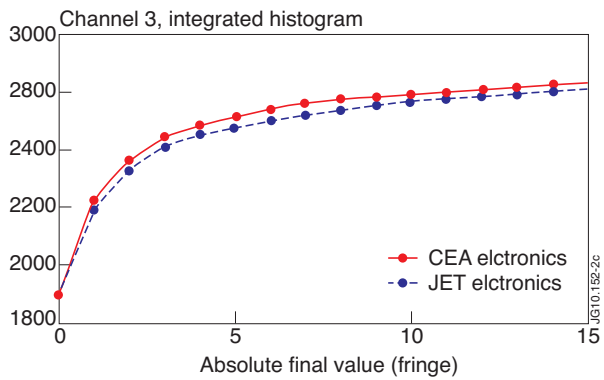


Figure 2: Statistics on 2755 plasma pulses.

Figure 3: Variation of the signal during an ELM.

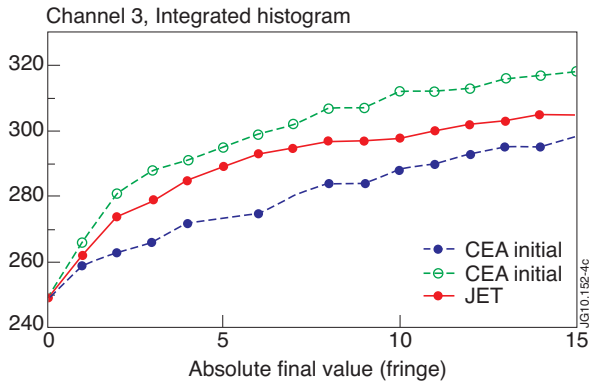


Figure 4: Diminution of the final phase by the improved algorithm based on the number of fringes counted after a pulse, which is indicative of the fringe jump correction efficiency.

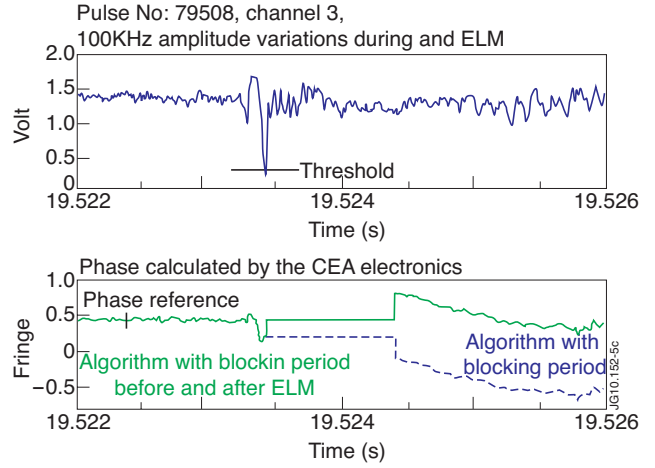


Figure 5: Validation of the improved algorithm on an ELM.

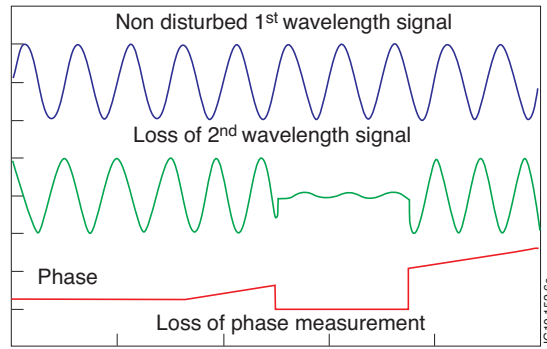


Figure 6: Signal loss of one of the wavelength signals.

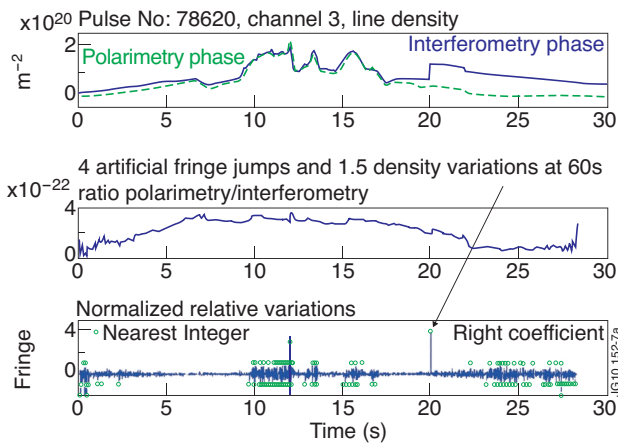


Figure 7: Time evolution of the normalised ellipticity.

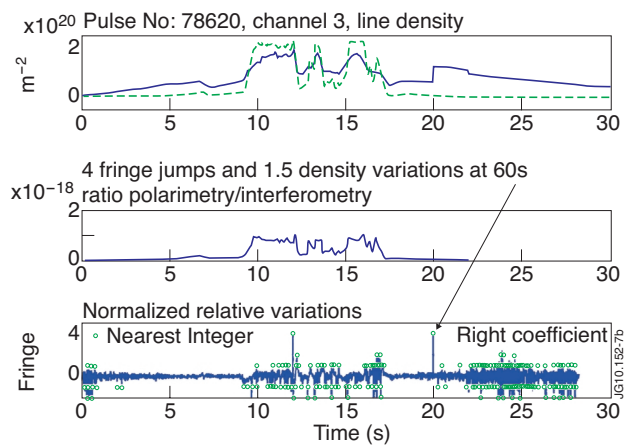


Figure 8: Time evolution of the normalised phases.